

DETERMINATION OF INDENTER CRACK PROBABILITY ON MULTILAYER STACKS USING AN ACOUSTIC EMISSION TEST METHOD

Marianne Unterreitmeier and Oliver Nagler
Infineon Technologies AG
marianne.unterreitmeier@infineon.com

INTRODUCTION

Acoustic emission (AE) testing is one of the most efficient and versatile techniques used for nondestructive testing (NDT) of materials. It can detect, localize, and monitor material defects during the entire system lifetime without any destruction of the specimen. During solid material fracturing, such as due to a mechanical load, the stored elastic energy is released suddenly, producing acoustic shock waves. For this purpose, AE sensors are physically coupled to the surface of the specimen to detect elastic waves, which are radiated spherically from the location of a spreading defect. The volume and surface waves propagate with ultrasonic frequencies (20 kHz – 2 MHz) at low amplitudes and short durations measured by piezoelectric sensors.^[1]

This method is widely used in various science and industry applications to study the formation and growth of cracks, delamination, or plastic deformation in mechanical structures. A special field of application for the AE test method includes semiconductor devices, which can be damaged during handling, testing, or dicing.

During semiconductor wafer probing each device under test (DUT) is mechanically contacted on its connection pads by elastic contact springs, or probes, of a probe card, and electrically connected to the automatic test equipment (ATE). The induced mechanical contact stress, however, can partially exceed the permissible yield. Brittle isolation layers below the pad may fracture, causing cracks, delamination, or deformation.

In the past, there were only destructive optical methods to detect cracks in brittle insulation layers. This kind of failure analysis, which is only applicable after wafer testing, is time consuming, destructive, and partly inaccurate. To detect material defects in multilayer semiconductor structures in real-time during wafer probing,

an innovative process based on AE testing was recently developed at Infineon Technologies AG.^[1,2]

This article explains the AE test method and crack-detection process first. Examples of applications for various semiconductor multilayer structures are described, and a new prediction model for the crack probability is presented, which can be applied for probing-induced failures of complex semiconductor pad stacks. This method is faster, more accurate, and widely applicable compared to classical failure analysis techniques.

ACOUSTIC EMISSION TEST METHOD APPLIED ON WAFER PROBING

During semiconductor wafer probing, elastic probes are pressed on the pad surface of integrated circuits (ICs), generating regions of high mechanical stress in thin-layer structures below the pad (see Fig. 1). At critical stress conditions, cracks in brittle layers are induced, releasing acoustic shock waves moving further into the body and onto the surface of the wafer. Probing induced inter-metal layer dielectric (IMD) cracks have sizes down to nanometer dimensions with very small released crack energy. This requires very high sensitivity and resolution of the AE measurement system and elimination of disturbances.^[1]

The elastic waves caused by acoustic events during contacting are transmitted into an AE sensor, which is normally glued below the chip backside (see Fig. 2, left). Most types of probes used for wafer probing generate a lateral force in addition to a vertical force. The lateral scrubbing motion, however, causes an acoustic noise which overlays with a possible oxide crack. Therefore, instead of a conventional spring-like cantilever needle, a rigid vertically arranged needle (indenter) is used, acting exclusively perpendicular to the test structure during the contact without causing a lateral scrub (see Fig. 2, right).

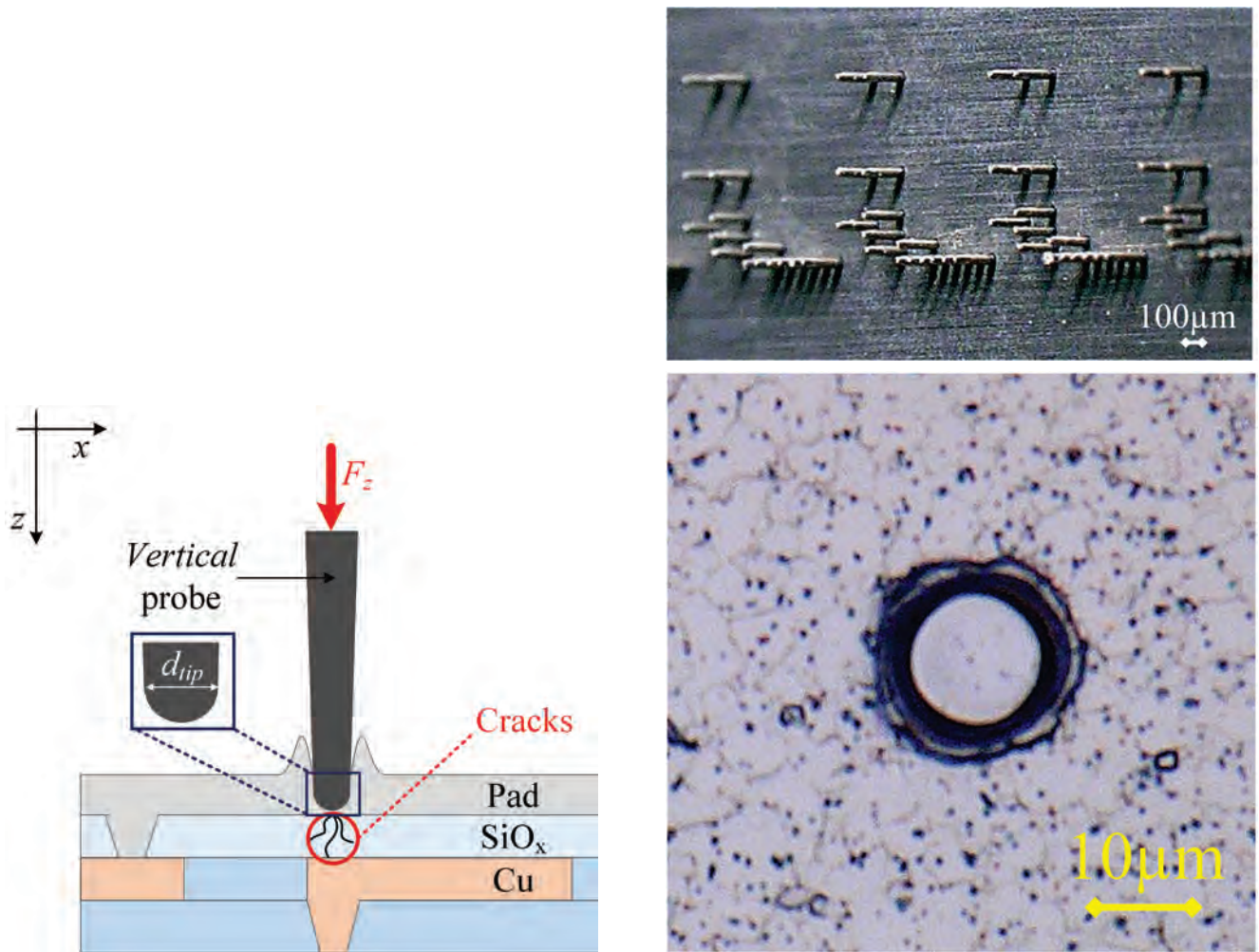


Fig. 1 Vertical probe contacting a CMOS technology pad stack and thereby inducing oxide cracks,^[1] left, vertical probes, right top, and imprint on Al-Cu top surface, right bottom.

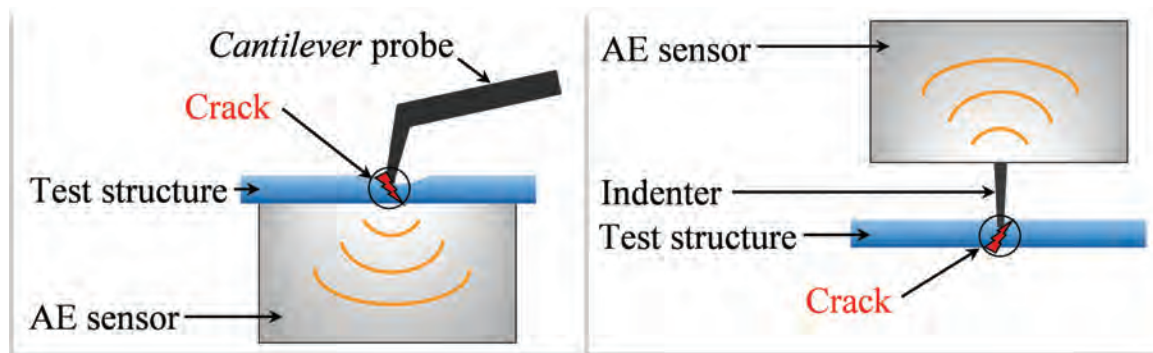


Fig. 2 Modification of the contact needle and sensor coupling concept.^[1]

In addition, instead of placing and gluing the test structure on the AE sensor (Fig. 2, left), the indenter is arranged vertically and directly coupled to the AE sensor (Fig. 2, right). This has the advantage that the acoustic wave is coupled at the location of the highest sensor sensitivity which is in the center of the cylinder surface. Moreover, the newly developed coupling concept eliminates the time-consuming and complicated gluing as well as removing of

the chip from the sensor which can cause a destruction of sensitive structures. This new concept better meets the requirements of the AE measurement in terms of stability, strength, and accuracy.

Fig. 3 shows the final prototype of the indenter glued on an AE sensor. This indenter design was successfully used in the following AE crack detection experiments.^[1]

For the AE crack detection experiments, a one-of-a-kind test bench called Probe Force Investigation Tool (PROFIT) was used (see Fig. 4). This platform, which was developed and assembled in-house at Infineon Technologies AG, enables time-synchronized measuring of both the contact force and AE signals during contacting of test structures with an indenter.

The test bench consists of several commercial instruments, which are connected by Ethernet interface and controlled by a LabVIEW program. One component is a three-axis motorized stage with a 200 mm wafer vacuum

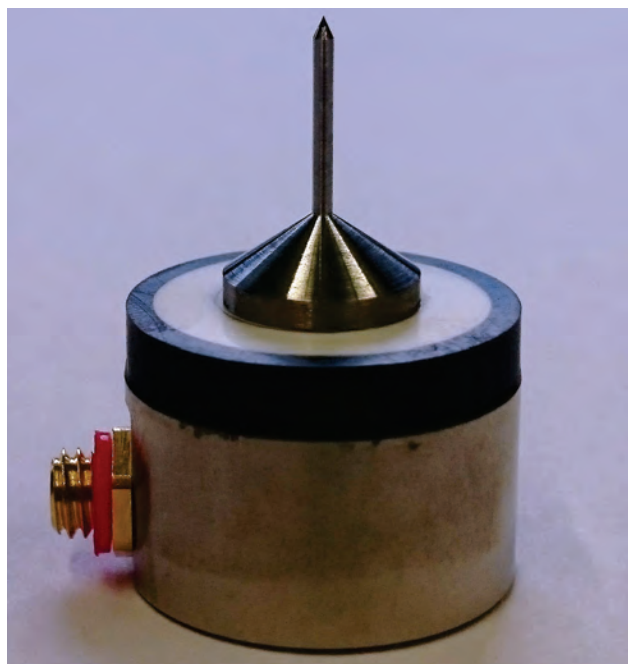


Fig. 3 Realized sensor-indenter system.^[1]

chuck on top. The stage controller unit, which is connected to the stages, provides an accurate positioning in x-, y-, and z-direction.

The sensor-indenter system is placed into an AE sensor holder and fixed by screws. The holder is connected to the DMS force sensor, which is assembled with a two-axis tilting stage to compensate a tilting error of the indenter relative to the surface of the test structure. The signal of the force sensor is fed into a force controller unit. The signal of the AE sensor is fed into a preamplifier, which is further connected to an AE controller unit. The voltage signal of the force sensor, which is converted into a calibrated contact force later, is measured parallel to the AE signals in time synchronization. Therefore, the analog signal of the force sensor is fed into the parametric input of the AE controller unit, where the synchronization takes place automatically.

To exactly position the indenter tip to the test structure, a camera alignment system is installed on the frame. The PROFIT is further equipped with a desktop PC including two monitors, a mouse, and a keyboard. The whole test bench is placed on a passive vibration isolation table to compensate external disturbances and shocks, which can generate errors in the sensitive AE measurement.

ACOUSTIC EMISSION CRACK DETECTION ON MULTILAYER STACKS

MULTILAYER STACK TEST SAMPLES

For the acoustic crack experiments various crack-sensitive test structures with alternating metal and oxide

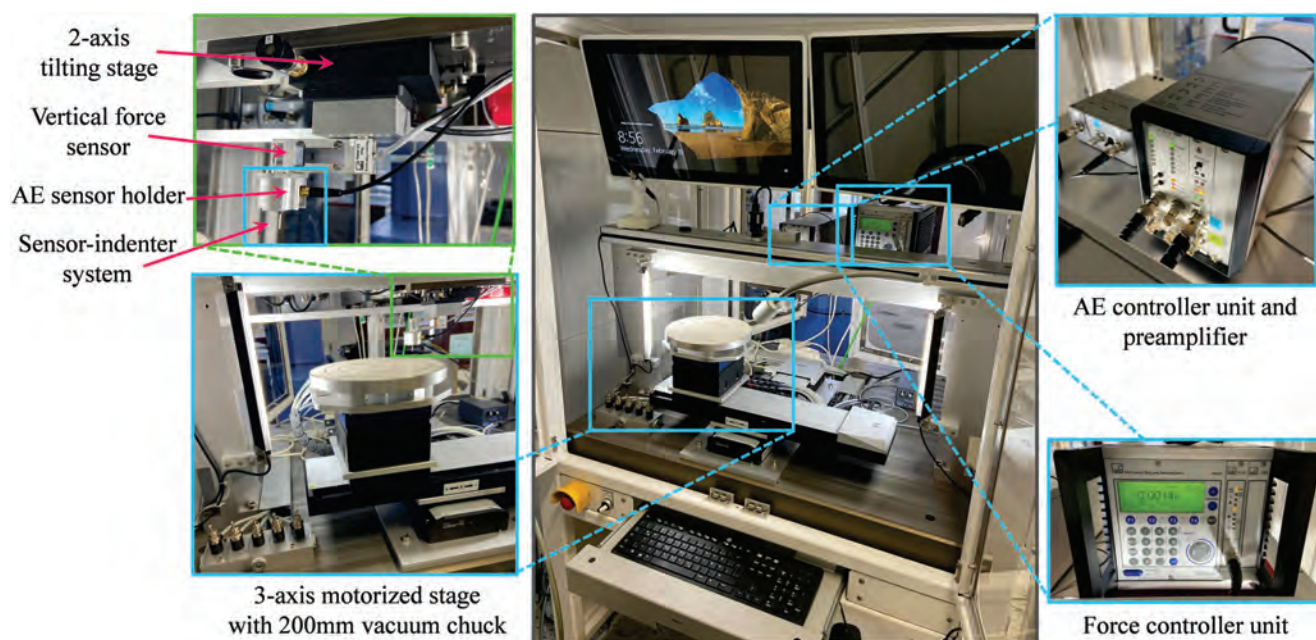


Fig. 4 Test bench PROFIT for AE crack experiments.

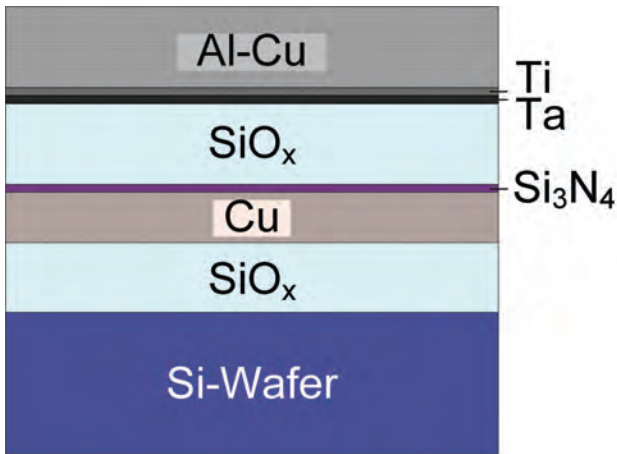
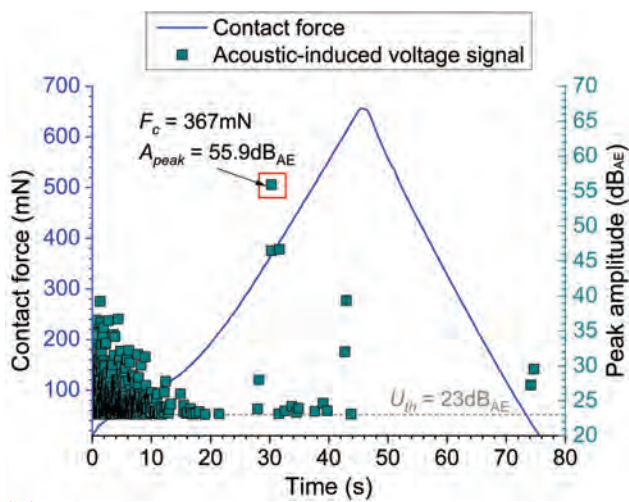


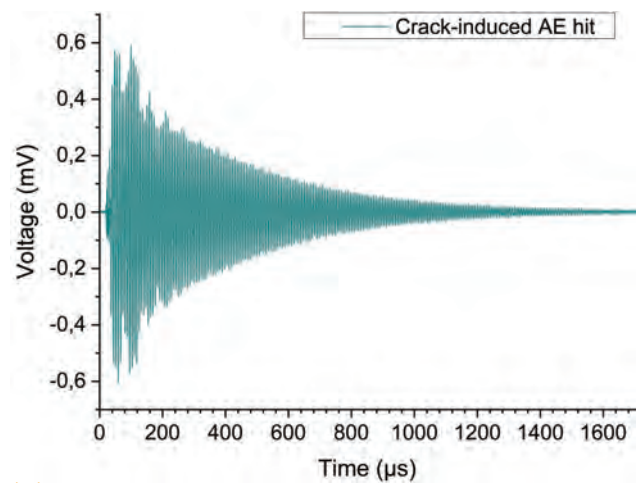
Fig. 5 Schematic layer stack of test structures W06, W08, and W11.^[1]

Table 1 Layer thicknesses of test structures W06, W08, and W11.

Test structure	W06	W08	W11
	Layer thickness, nm		
Al-Cu	1450	1450	3000
Ti	40	40	40
Ta	50	50	50
SiO _x	1000	1000	3000
Si ₃ N ₄	50	50	50
Cu	700	400	700
SiO _x	1900		
Si-wafer	500 × 10 ³		



(a)



(b)

Fig. 6 (a) Contact cycle on test structure W11 using indenter FP10,^[1] (b) acoustic-induced voltage signal by an oxide crack.

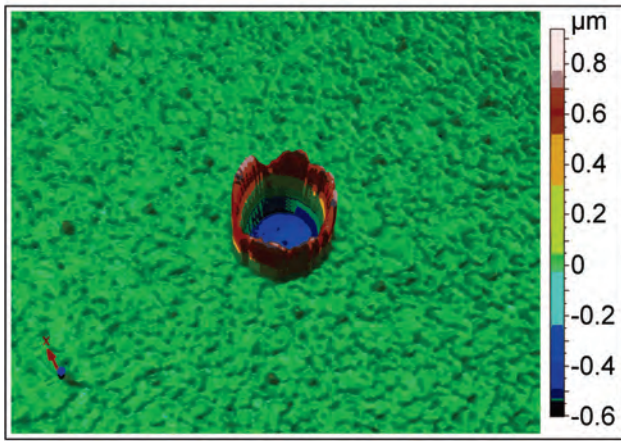
layers were processed on a silicon wafer (see Fig. 5). The test samples differ either in the thickness of the aluminum-copper (Al-Cu), the upper silicon oxide (SiO_x), or the copper (Cu) layer (see Table 1). In order to assess the crack probability for semiconductor devices, the design and material of the test structures are similar to typical back-end-of-line (BEOL) layer stacks of CMOS technology chips.

EXPERIMENTAL SETUP AND DATA PROCESSING

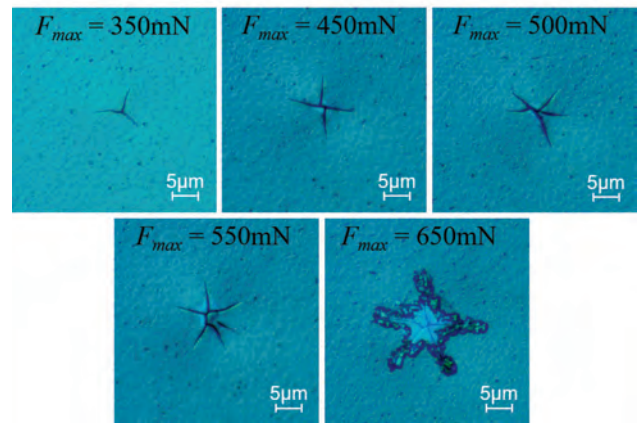
In this study, the AE crack experiments were performed using an indenter with a flat-ended circular diamond tip of 5 or 10 μm in diameter (abbreviated FP05 and FP10, respectively), which is pressed vertically on top of the surface of the test structure, analog to a realistic probing process.

Figure 6a shows a typical contact cycle for contacting an Al-Cu top layer. In this experiment, test structure W11 was loaded up to a maximum contact force of 650 mN using the indenter FP10 and subsequently unloaded (blue

curve). The associated acoustic-induced voltage signals are shown as green dots, the so-called AE hits. The peak amplitude of each hit is plotted in dB_{AE} (reference value 1 μV). In the given example, the time-dependent force curve is nonlinear up to a contact force of approximately 230 mN, while simultaneously numerous AE hits were measured above a threshold voltage U_{th} of 23 dB_{AE}. This effect is caused by the fact that the indenter penetrates with rising contact load into the Al-Cu top layer, which is plastically deformed and the indentation depth is increasing (see Fig. 7a). The number of AE hits and their peak amplitude is decreasing proportional to the increasing penetration depth. Above a contact force of 230 mN only isolated hits of low amplitude occur. The cracking of the SiO_x layer during indentation on the Al-Cu top layer starts at a contact force F_c of 367 mN with a peak amplitude A_{peak} of 55.9 dB_{AE}. An exemplary wave signal of a crack-induced AE hit is plotted in Fig. 6b, over its whole signal duration time.^[1]



(a)



(b)

Fig. 7 (a) Measuring the imprint depth after Al-Cu indentation using a confocal microscope. (b) Differential interference contrast (DIC) microscopy images of oxide cracks after indentation on Al-Cu top layer and chemical crack preparation at different maximum contact forces.^[1]

In this work, the burst-signal energy is used to filter the measured AE signals. Using this AE feature, the crack signals are clearly distinguishable from other signals, like plastic deformation, in terms of higher amplitudes and signal lengths. The burst-signal energy E_{burst} is calculated from the sum of all squared voltage samples U_i of a hit ($i = 1, 2 \dots n$) multiplied by the sampling time interval T_s and has the unit eu ($1 \text{ eu} = 10^{14} \text{ V}^2\text{s}$).^[1]

$$E_{burst} = \sum_{i=1}^{i=n} U_i^2 T_s$$

To identify the correct filter criteria for the “first oxide cracks,” 100 contact cycles were performed sequentially on test structure W11. The test structure was again stressed for each contact cycle up to a max. contact force of 650 mN to achieve nearly 100% crack probability in combination with indenter FP10. Figure 8 shows a scatter plot of the burst-signal energy in logarithmic scale for all recorded AE hits as a function of the contact force cumulated for 100 contact cycles.

The burst-signal energy and the number of measured AE hits are relatively high at low contact forces. With increasing contact force, the burst-signal energy is getting lower, while the imprint depth increases. This effect can be explained by weakening of the plastic deformation of the Al-Cu top layer at higher forces. After the imprint depth saturation region between a contact force of approximately 200 and 280 mN, the burst-signal energy of the AE hits is rising again, while the contact force is continuously increased. As shown in Fig. 8, the oxide crack generation starts above a force value of approximately 280 mN. The occurrence of cracks within the range of critical contact force is also confirmed by optical inspections (see Fig. 7b).

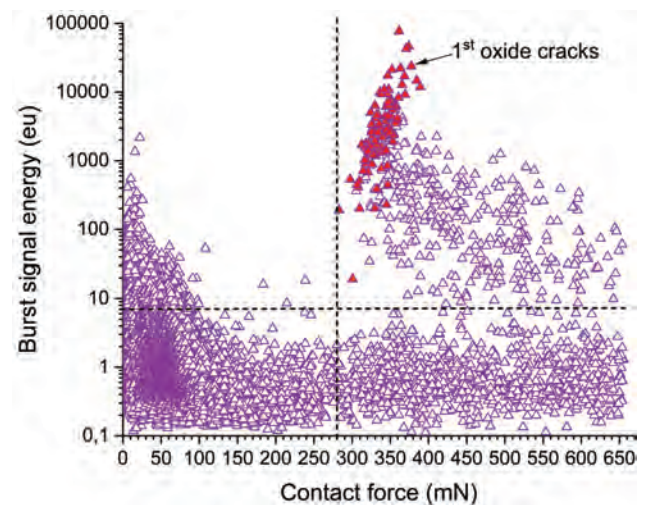


Fig. 8 Burst-signal energy of all hits recorded for 100 contact cycles on test structure W11 using indenter FP10 as function of contact force (all triangles) and clustering of AE signals regarding first oxide cracks (triangles marked in red).

In this experiment, the lower filter limit of the burst-signal energy is set to 7 eu and for the contact force it is set to 280 mN. Only AE hits meeting these filter criteria are considered and utilized for further data evaluation.

After filtering the data from Fig. 8, only those hits are selected that have occurred for the first time per indent, so-called “first oxide cracks.” The critical contact forces are statistically evaluated from the remaining data points. Figure 9 shows the result for all 100 contact cycles as a histogram plot over the contact force. The graph also shows the distribution function as a blue line, which has been fitted to the data points.

The distribution function graph is not symmetrical, as the maximum count of AE hits is shifted slightly to the right.

This hints at the suggestion that the crack probability is not normal, but Weibull-distributed. Assuming that, the force-dependent crack probability of multilayer stacks follows a two-parametric Weibull distribution function P_f of the form:

$$P_f(F) = 1 - e^{-\left(\frac{F}{F_{\text{char}}}\right)^m}$$

with the Weibull modulus (or slope) m and the characteristic contact force F_{char} .

It can be seen from the curve of the distribution function, that the maximum frequency of cracks occurs at a contact force of approximately 345 mN. By definition, this corresponds to the characteristic contact force F_{char} with 63% crack probability and confirms the theory that critical forces causing cracks in brittle materials follow a Weibull distribution.

Figure 10 shows the cumulative probability of first oxide cracks in Weibull scale as a function of the contact force. From this plot the Weibull modulus m is graphically derived from the linear regression line with a value of 18.3 and the characteristic contact force F_{char} is 347 mN. According to statistical analysis, the distribution of the data points follows a Weibull distribution at a significance level of 0.05.

At contact forces below 320 mN, however, the filtered data points are no closer to the linear regression line (green line) and are below the confidence band (red lines). The two-parametric Weibull distribution function does not accurately describe the crack probability here. The next section gives a hypothesis to improve the crack probability model.

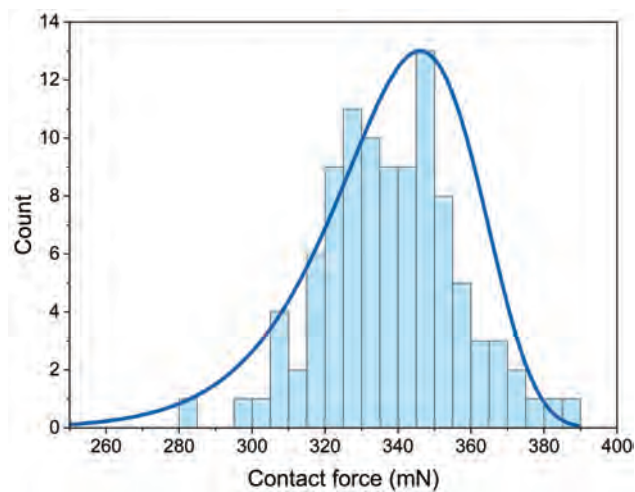


Fig. 9 Histogram of first oxide cracks for 100 contact cycles on test structure W11 using indenter FP10 as function of contact force, bin size 5 mN.

HIGH-STATISTIC CRACK PROBABILITY ASSESSMENT FOR DIFFERENT LAYER STACKS

To further prove the crack probability assessment for a higher sample size using the AE test method and to verify the two-parametric Weibull distribution model, two further AE indenter measurements were performed on test structure W06 and W08 using the indenter FP05 (tip diameter: 5 μm). For each test structure, 1000 successive contact cycles were performed at contact stress levels, which were high enough to reach a crack probability of approximately 100%. Following the experiments, a statistical data analysis was carried out. The result of the cumulative crack probability in Weibull scale is shown in Fig. 11.

Based on the results of the crack probability measurement on test structure W08, which has a 400 nm Cu layer below the upper SiO_x layer, the characteristic contact force F_{char} is 22.2 mN higher compared to test structure W06 (700 nm Cu layer). This result agrees well with the findings in Unterreitmeier,^[1] stating that the characteristic contact force increases with decreasing Cu layer thickness. The Weibull modulus m for test structure W08 is smaller compared to structure W06, meaning that the scatter of the recorded AE crack signals for test structure W08 is lower compared to structure W06. Obviously a thicker Cu layer below the oxide layer is negatively affecting both the robustness and the reliability of the layer stack.

Based on statistical calculations, the measurement points of both test structures follow a two-parametric Weibull distribution at a significance level of 0.05. For test

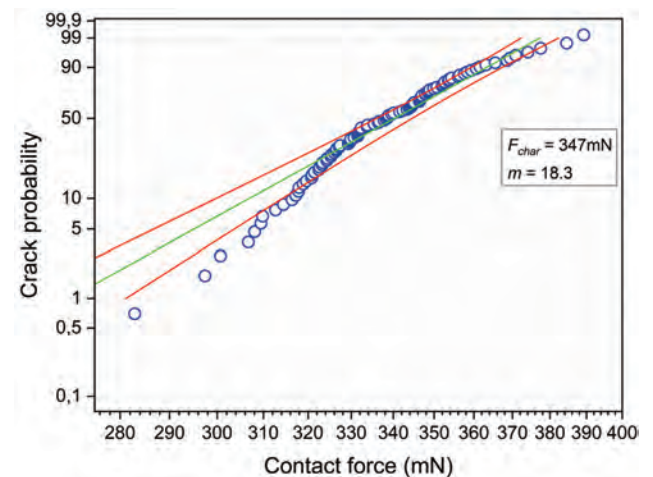
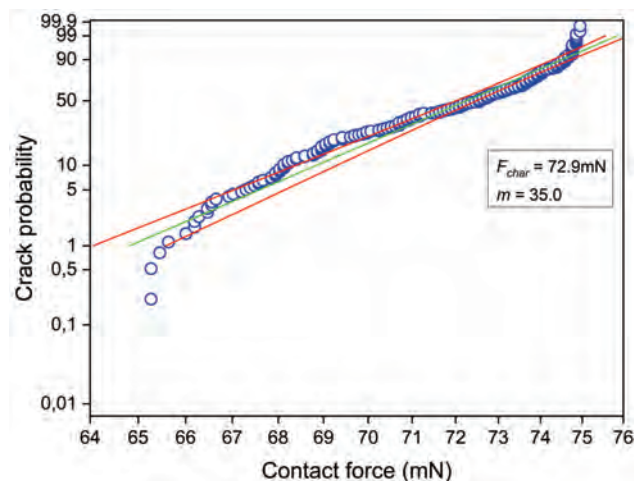


Fig. 10 Cumulative probability of first oxide cracks for 100 contact cycles on test structure W11 using indenter FP10 in Weibull scale as function of contact force (linear regression line: green, 95% confidence band: red).

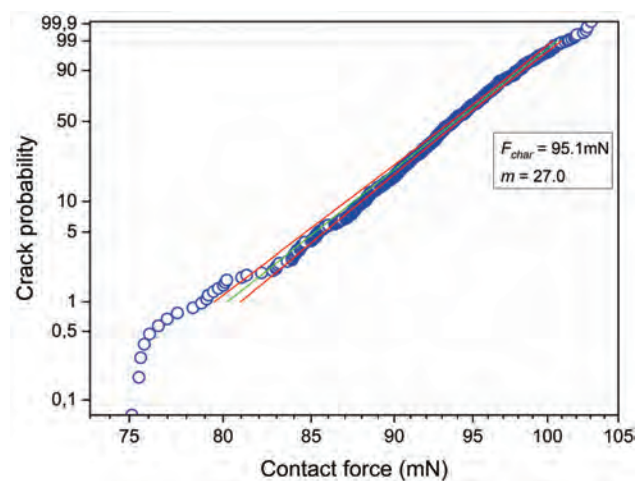
structure W08 the measurement points are within the 95% confidence band for contact forces higher than 82 mN, denoting the high precision of the new AE test method. Also for test structure W06 the measurement points are close to the linear regression line for forces higher than

66 mN. However, as in the example before, below these contact forces, the measurements points do not follow well the linear regression line.

This observation leads to a new hypothesis in order to improve the model for the crack probability during



(a)



(b)

Fig. 11 Cumulative probability of first oxide cracks for 1000 contact cycles on test structure W06 (a) and W08 (b) using indenter FP05 in Weibull scale as function of contact force (linear regression line: green, 95% confidence band: red).

Providing Microscopy Supplies and Specimen Preparation Equipment to Our Valued Customers in Materials Science for Over Half a Century



PELCO® Dimpler™

Precision electronic device delayering and specimen thinning for electron microscopy



PELCO® Precision Wire Saw

Precision cutting for delicate samples using gentle lapping action



PELCO® Precision Low Speed Saw

Multipurpose, low-damage cutting for all specimen types



Lapping & Thinning Fixtures

Preparation by hand to a specific plane of interest for TEM or SEM



Lapping Film

Available in a wide range of abrasive sizes



PELCO® FIB Lift-Out Grids

Indicator Grids for TEM, 5 or 8 narrow post, copper



Wafer Carriers & Holders

Available in all common wafer sizes

TED PELLA, INC.
Microscopy Products for Science and Industry

www.tedpella.com sales@tedpella.com 800.237.3526

indentation on multilayer stacks by a three-parametric Weibull distribution. Additional to the Weibull slope m and shape, which is here the characteristic force F_{char} , a third parameter γ , the so-called location parameter, is introduced. This improved distribution function considers the physical behavior of thin layers, which have a lower fractural stress limit, where no cracks occur.

CONCLUSION

This article presented a novel AE test method to detect cracks in brittle semiconductor layers during contacting by pointed tip indenters. The process is similar to wafer probing and can be used to characterize the mechanical robustness of multilayer stacks. Additional to the test bench setup, the measurement concept was discussed and the data analysis process explained. Three examples demonstrated the capability for crack probability assessments.

The accuracy of the AE test method was correlated by conventional failure analysis methods. It was proven that a highly accurate, reliable, and efficient detection of oxide cracks using the AE test method is possible even in the

nanometer scale dimension. So in the future, this method can be applied to characterize semiconductor BEOL stacks for probing and other stress-related processes during the manufacturing flow.

Furthermore, the results have shown that the two-parametric Weibull distribution function does not accurately describe the crack probability for thin, brittle layers. This observation leads to a new hypothesis to improve the model for the crack probability during indentation on multilayer stacks by a three-parametric Weibull distribution. Further investigations are continuing at Infineon Technologies AG to prove this hypothesis.

REFERENCES

1. M. Unterreitmeier: "Contact Related Failure Detection of Semiconductor Layer Stacks using an Acoustic Emission Test Method," FAU Forschungen, Reihe B, Medizin, Naturwissenschaft, Technik Band 33, FAU University Press, Erlangen, Germany, 2020, DOI: 10.25593/978-3-96147-306-9.
2. M. Unterreitmeier, et al.: "An Acoustic Emission Sensor System for Thin Layer Crack Detection," *Microelectronics Reliability*, 2018, Vol. 88-90, p. 16-21.

ABOUT THE AUTHORS



Marianne Unterreitmeier studied renewable energies – electrical engineering (B.Eng.) and micro- & nanotechnology (M.Sc.) at the University of Applied Sciences in Munich. She received her master's degree in 2016 with two awards: "Oskar-von-Miller Award 2016 for Excellent Academic Achievement" and "University Award 2016 for Best Degree in Micro- & Nanotechnology." During her studies, she was a part-time working student at ZAE Bayern in Munich. Later, she moved to Infineon Technologies in Munich for her master's thesis on wafer test. Subsequently, she accepted an offer there for her doctoral research study in the field of acoustic event monitoring in cooperation with the FAU Erlangen-Nuremberg, OTH Regensburg. Unterreitmeier achieved the Best Paper Award at the ESREF 2018 conference in Aalborg, completed her Ph.D. work in 2019 with honors, and won the Regensburger Award for Women in Science and Art in 2021. She is still enthusiastic for her research topic and happy to continue as a permanent employee at Infineon's Test Technology and Innovation department.

Oliver Nagler finalized his diploma degree (Dipl.-Ing.) of aerospace engineering at the Technical University of Munich in 1994 and received his physical doctorate degree (Dr.-Ing.) in electrical engineering from the Bundeswehr Universität Munich in 2008. He started his career as a research engineer at the Fraunhofer Institut for Solid State Technology in Munich in 1995. Since 1999, he's been an employee at Infineon Technologies AG, Neubiberg, Germany, currently in the department of Test Technology and Innovation. He is a lead principal for wafer test technologies and head of Infineon's R&D probing lab. Nagler holds several patents and international publications in probing technology and processes including acoustic emission test method. In cooperation with national and international universities, he is regularly supervising bachelor, master, and Ph.D. students.

